Article

Cell Reports

Dysregulation of RBFOX2 Is an Early Event in Cardiac Pathogenesis of Diabetes

Graphical Abstract

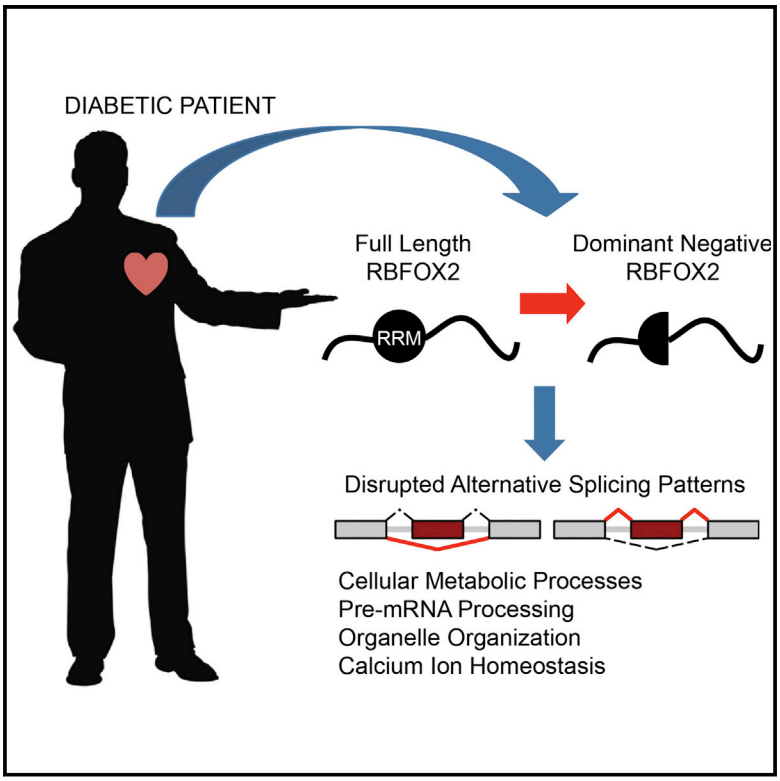

Authors

Curtis A. Nutter, Elizabeth A. Jaworski, Sunil K. Verma, ..., Xander H.T. Wehrens, Gene W. Yeo, Muge N. Kuyumcu-Martinez

Correspondence

nmmartin@utmb.edu

In Brief

Nutter et al. show that the majority of transcripts mis-spliced in diabetic hearts have RBFOX2-binding sites. In diabetic hearts, a DN isoform of RBFOX2 with inhibitory splicing function is generated in response to high protein levels of WT RBFOX2. DN RBFOX2 upregulation occurs before cardiac complications manifest.

Highlights

- 73% of transcripts mis-spliced in diabetic hearts have RBFOX2-binding sites
- RBFOX2 AS function is modulated in diabetic hearts via a DN isoform
- DN RBFOX2 expression precedes diabetic cardiac complications
- DN RBFOX2 delays intracellular calcium transients in cardiomyocytes

Accession Numbers

GSE80664

Nutter et al., 2016, Cell Reports *15*, 1–14
June 7, 2016
http://dx.doi.org/10.1016/j.celrep.2016.05.002

CellPress

Please cite this article in press as: Nutter et al., Dysregulation of RBFOX2 Is an Early Event in Cardiac Pathogenesis of Diabetes, Cell Reports (2016), http://dx.doi.org/10.1016/j.celrep.2016.05.002

Cell Reports
Article

Dysregulation of RBFOX2 Is an Early Event in Cardiac Pathogenesis of Diabetes

Curtis A. Nutter,[1] Elizabeth A. Jaworski,[1] Sunil K. Verma,[1] Vaibhav Deshmukh,[2] Qiongling Wang,[2,3] Olga B. Botvinnik,[4] Mario J. Lozano,[5] Ismail J. Abass,[6] Talha Ijaz,[1] Allan R. Brasier,[6,7] Nisha J. Garg,[8,9,11] Xander H.T. Wehrens,[2,3,12,13] Gene W. Yeo,[4,14] and Muge N. Kuyumcu-Martinez[1,7,10,*]

[1]Department of Biochemistry and Molecular Biology, University of Texas Medical Branch, Galveston, TX 77555, USA
[2]Department of Molecular Physiology and Biophysics, Baylor College of Medicine, Houston, TX 77030, USA
[3]Cardiovascular Research Institute, Baylor College of Medicine, Houston, TX 77030, USA
[4]Department of Cellular and Molecular Medicine, University of California San Diego, La Jolla, CA 92037, USA
[5]Department of Biological Sciences, University of Texas at Dallas, Richardson, TX 75080, USA
[6]Department of Internal Medicine, University of Texas Medical Branch, Galveston, TX 77555, USA
[7]Institute for Translational Sciences, University of Texas Medical Branch, Galveston, TX 77555, USA
[8]Department of Microbiology and Immunology, University of Texas Medical Branch, Galveston, TX 77555, USA
[9]Department of Pathology, University of Texas Medical Branch, Galveston, TX 77555, USA
[10]Department of Neuroscience and Cell Biology, University of Texas Medical Branch, Galveston, TX 77555, USA
[11]Institute for Human Infections and Immunity, University of Texas Medical Branch, Galveston, TX 77555, USA,
[12]Department of Medicine/Cardiology, Baylor College of Medicine, Houston, TX 77030, USA
[13]Department of Pediatrics, Baylor College of Medicine, Houston, TX 77030, USA
[14]Institute for Genomic Medicine, University of California San Diego, La Jolla, CA 92037, USA
*Correspondence: nmmartin@utmb.edu
http://dx.doi.org/10.1016/j.celrep.2016.05.002

SUMMARY

Alternative splicing (AS) defects that adversely affect gene expression and function have been identified in diabetic hearts; however, the mechanisms responsible are largely unknown. Here, we show that the RNA-binding protein RBFOX2 contributes to transcriptome changes under diabetic conditions. RBFOX2 controls AS of genes with important roles in heart function relevant to diabetic cardiomyopathy. RBFOX2 protein levels are elevated in diabetic hearts despite low RBFOX2 AS activity. A dominant-negative (DN) isoform of *RBFOX2* that blocks RBFOX2-mediated AS is generated in diabetic hearts. DN *RBFOX2* interacts with wild-type (WT) RBFOX2, and ectopic expression of DN RBFOX2 inhibits AS of RBFOX2 targets. Notably, DN *RBFOX2* expression is specific to diabetes and occurs at early stages before cardiomyopathy symptoms appear. Importantly, DN RBFOX2 expression impairs intracellular calcium release in cardiomyocytes. Our results demonstrate that RBFOX2 dysregulation by DN RBFOX2 is an early pathogenic event in diabetic hearts.

INTRODUCTION

Diabetic patients have a 2- to 5-fold increased risk of developing cardiovascular diseases, which include atherosclerosis, hypertensive heart disease, and diabetic cardiomyopathy (Trachanas et al., 2014). Cardiovascular complications are the number one cause of mortality and morbidity among diabetic patients (Ferrannini and Cushman, 2012; Harcourt et al., 2013). Diabetic cardiomyopathy is particularly difficult to manage due to its asymptomatic nature and its ability to progress into heart failure (Aneja et al., 2008; Asghar et al., 2009; Boudina and Abel, 2010). The molecular mechanisms responsible for diabetic cardiomyopathy are poorly understood, though chronic activation of protein kinase C (PKC) signaling has been implicated in the pathogenesis (Geraldes and King, 2010; Inoguchi et al., 1992; Liu et al., 2009). Inhibition of PKC activity improves cardiac complications in animal models of diabetes (Connelly et al., 2009; Liu et al., 2012) by mechanisms that are not well defined.

We have previously shown that PKC activation leads to reactivation of fetal alternative splicing (AS) programs in diabetic hearts partly via phosphorylation of the RNA-binding protein RBFOX2 (Verma et al., 2013). Consistent with this finding, we have shown that RBFOX2 protein levels are elevated in diabetic mouse hearts (Verma et al., 2013), suggesting a role for RBFOX2 in the pathogenesis of diabetes. In this study, we wanted to further investigate how RBFOX2 regulation is modulated in diabetic hearts and whether changes in RBFOX2 contribute to aberrant AS in diabetes.

RBFOX2 directly binds to the consensus (U)GCAUG motif in target pre-mRNAs and regulates AS in a position-dependent manner. Binding to the downstream intron induces alternative exon inclusion, but binding to the upstream intron triggers exon exclusion (Huang et al., 2012; Sun et al., 2012; Yeo et al., 2009). Genome-wide RBFOX2 target pre-mRNAs have been identified using cross-linking IP followed by RNA sequencing (CLIP-seq) analysis in human and mouse embryonic stem cells (ESCs) and human 293T cells (Jangi et al., 2014; Lovci et al.,

Please cite this article in press as: Nutter et al., Dysregulation of RBFOX2 Is an Early Event in Cardiac Pathogenesis of Diabetes, Cell Reports (2016), http://dx.doi.org/10.1016/j.celrep.2016.05.002

2013; Yeo et al., 2009). RBFOX2 controls the expression of other RNA-binding proteins via AS-induced nonsense-mediated mRNA decay (Jangi et al., 2014; Yeo et al., 2009). Therefore, RBFOX2 affects gene expression at multiple levels, either directly or indirectly via modulating other RNA-binding proteins.

RBFOX2 is implicated in several cellular processes such as apoptosis, proliferation, and epithelial-mesenchymal transition (Baraniak et al., 2006; Gehman et al., 2012; Venables et al., 2013a). RBFOX2 is necessary for the survival of ESCs (Yeo et al., 2009) and brain development (Gehman et al., 2012). It also plays an important role in differentiation of pluripotent stem cells (Venables et al., 2013b). A recent study has shown that RBFOX2 is implicated in pressure-overload-induced heart failure (Wei et al., 2015). However, its role in diabetes is unknown.

In this study, we show that 704 alternative exons differentially spliced in diabetic hearts are RBFOX2 targets. We find that RBFOX2 regulates AS of transcripts with validated RBFOX2-binding sites. Results indicate that AS changes in RBFOX2 targets are due to low RBFOX2 levels or activity in diabetic hearts. However, RBFOX2 protein levels are paradoxically elevated in type 2 diabetic (T2D) human patients' hearts. Our results reveal that the mechanism for low RBFOX2-dependent AS in diabetes is due to the increased expression of a dominant-negative (DN) isoform of *RBFOX2*, which possesses an inhibitory AS function. DN *RBFOX2* is expressed early in response to high glucose levels in diabetic mice and is specific to diabetic complications in the heart. We show that DN *RBFOX2* generation in diabetic hearts is dependent on upregulation of RBFOX2 protein with intact RNA-binding capability. Overexpression of DN RBFOX2 inhibits AS of RBFOX2 targets and impairs intracellular calcium handling in cardiomyocytes. Finally, our data indicate that DN RBFOX2 binds to wild-type (WT) RBFOX2 as a likely mechanism to repress RBFOX2 splicing function. In sum, our results demonstrate that dysregulation of RBFOX2 activity triggers AS abnormalities and contributes to diabetic complications in the heart.

RESULTS

RBFOX2-Binding Sites Are Enriched in Pre-mRNAs that Undergo AS Changes in Diabetic Hearts

We have previously identified genome-wide AS changes in type 1 diabetic (T1D) mouse hearts with a corresponding increase in RBFOX2 protein levels (Verma et al., 2013). Therefore, we hypothesized that RBFOX2 is involved in AS dysregulation in diabetic hearts. Because genome-wide RBFOX2-binding sites were determined using human ESCs by CLIP-seq (Yeo et al., 2009), we wanted to determine whether transcripts mis-spliced in diabetic mouse hearts have RBFOX2-binding sites. To this end, we mapped the human RBFOX2-binding sites to the corresponding mouse genomic coordinates. Seventy-three percent of total pre-mRNAs mis-spliced in diabetic hearts displayed RBFOX2-binding clusters within alternative exons and introns (adjacent 500 nt; Figure 1A). For controls, transcripts with similar expression levels but that did not display splicing changes in diabetic hearts were used. The majority (1,023 out of 1,417) of RBFOX2-binding clusters were located within introns (Figure 1B) consistent with the role of RBFOX2 in AS regulation. RBFOX2-binding clusters within intronic regions of mis-spliced transcripts were statistically significant when compared to binding clusters within control transcripts (Figures 1B and S1). To determine the functions of the affected RBFOX2 target genes in diabetic hearts, we performed gene ontology analysis using the NIAID Database for Annotation, Visualization and Integrated Discovery (DAVID) server using the whole genome as a background control. RBFOX2 target genes dysregulated in diabetic hearts have important biological functions in macromolecular metabolism, apoptosis, vesicular transport, calcium homeostasis, and cell cycle (Figure 1C).

RBFOX2 Regulates AS Events Mis-spliced in Diabetic Hearts

Next, we wanted to determine whether RBFOX2 regulates AS of the pre-mRNAs with RBFOX2-binding sites. We validated 22 out of 24 tested AS events identified by RNA-seq in T1D diabetic mouse hearts and 8 out of 11 tested AS events in T2D human hearts (data not shown). We further focused on a few AS events based on the criteria that (1) there is a significant AS change (>20%) in diabetic hearts, (2) AS removes a functional protein domain (Figure 1D), (3) the genes play important roles in heart function and disease (Figure 1D): *MTMR3* (Lorenzo et al., 2006; Taguchi-Atarashi et al., 2010); *FXR1* (Blackwell et al., 2010; Kirkpatrick et al., 1999; Mientjes et al., 2004; Whitman et al., 2011); *MEF2A* (Mora and Pessin, 2000; Naya et al., 2002; Wang et al., 2003; Weng et al., 2005; Zhu et al., 2005); and *PBX3* (Arrington et al., 2012; Monica et al., 1991; Stankunas et al., 2008), and (4) pre-mRNAs display distinct RBFOX2-binding sites in upstream or downstream intronic regions (Figure 1E). By examining the AS of these specific exons with intronic RBFOX2-binding sites (Figure 1E), we would be able to assess whether increased RBFOX2 levels correspond to diabetes-induced AS changes in the heart.

We tested AS of these four pre-mRNAs (*MTMR3* exon 16, *FXR1* exon 15+16, *MEF2A* exon 9, and *PBX3* exon 7) in T2D human hearts as well as in obese and hypertensive mouse models using qRT-PCR. Obesity and hypertension are common among diabetic patients, so we wanted to determine whether AS changes are induced by one of these factors under diabetic conditions. *MTMR3* exon 16, *FXR1* exon 15+16, *MEF2A* exon 9, and *PBX3* exon 7 were skipped more in T2D human patients' hearts compared to non-diabetic control human hearts, similar to the results in T1D mice (Figure 2A; Verma et al., 2013). However, none of these AS events changed in obese, hypertensive, or obese-hypertensive mice (Figures 2B and S2). Mice infused with angiotensin II had hypertrophic hearts, and obese mice were two times heavier than the controls (Figures 2C and 2D; Tieu et al., 2009). These data suggest that diabetes-induced AS changes are independent of hypertension or obesity status. We tested these AS events in mice with advanced cardiomyopathy and heart failure in order to determine whether AS changes are due to non-specific effects from failing hearts. None of the AS events was altered in chagasic mice with chronic cardiomyopathy and heart failure (Figure 2E; Gupta et al., 2015), indicating that AS changes were not due to sick hearts. Importantly, the alternative exons with downstream RBFOX2-binding sites were excluded in diabetic patients, suggesting low RBFOX2 levels or AS activity under diabetic conditions.

A

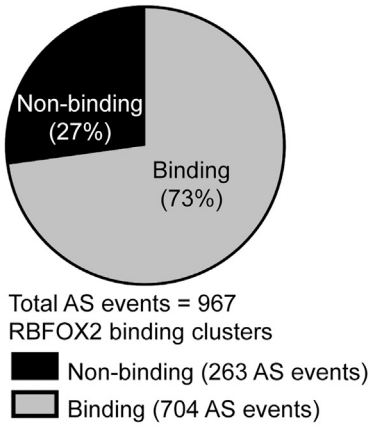

B

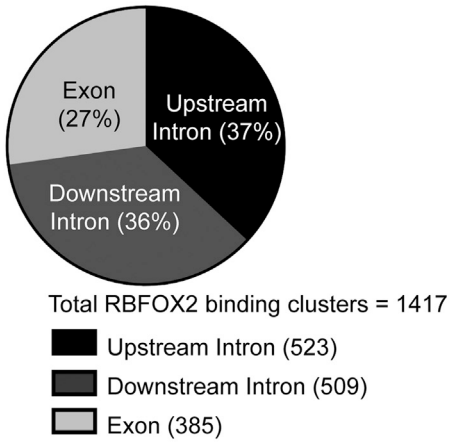

C

Category	Term	Count	P-Value
GOTERM_BP_ALL	Cellular metabolic process	228	1.5E-10
	Organelle organization	68	4.9E-10
	Chromatin organization	30	3.1E-8
	Post-translational protein modification	53	5.1E-5
PANTHER_BP_ALL	Pre-mRNA processing	23	7.5E-6
	Intracellular protein traffic	48	1.9E-5
	General vesicle transport	14	1.7E-2
	Chromatin packaging and remodeling	11	2.1E-2
	Apoptosis	22	3.2E-2
	Oncogenesis	19	4.1E-2
	Calcium ion homeostasis	4	6.7E-2

D

Gene	*MTMR3*	*FXR1*	*MEF2A*	*PBX3*
Molecular function	Protein Phosphatase	Translational Control	Transcription Factor	Transcription Factor
Protein domain affected by splicing in diabetes	Zinc finger motif (FYVE)	RNA-specificity domain (striated muscle specific)	Transactivation Domain	Transcriptional repression domain
Known associations with heart disease	Related to myotubularin gene that causes myopathy when mutated	Cardiomyopathy and heart failure	Myocardial infarction and glucose transport	Congenital heart defects

E

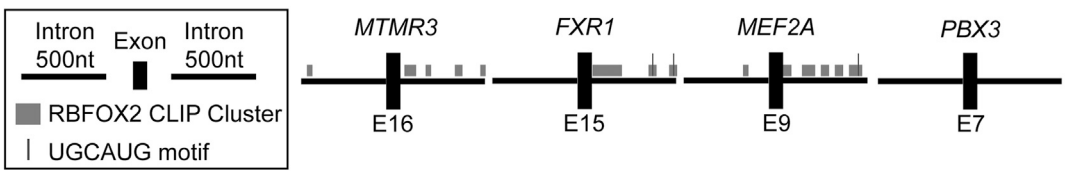

Figure 1. Seventy-Three Percent of Transcripts Aberrantly Spliced in Diabetic Mouse Hearts Have RBFOX2-binding Sites

(A) Pie chart of RBFOX2-binding clusters in 967 transcripts that are mis-spliced in type 1 diabetic (T1D) mouse hearts. Alternative splicing (AS) events affected in diabetic hearts with at least one CLIP peak at a Bayes factor ≥ 1 were designated as "significant" and <1 as "not significant."

(B) RBFOX2-binding site distribution among 1,417 RBFOX2-binding clusters within 704 pre-mRNAs aberrantly spliced in diabetic hearts (see Figure S1).

(C) Top gene ontology categories for RBFOX2-regulated genes affected in diabetic hearts. DAVID server was used to categorize genes based on biological or molecular function. p values represent statistical significance when compared to the whole genome, which was used as a background control.

(D) Effect of diabetes-induced AS changes on gene expression and function.

(E) Schematic of intronic RBFOX2-binding sites obtained from human ESC RBFOX2 CLIP-seq data with CLIP clusters and consensus RBFOX2-binding site motif (U)GCAUG on target pre-mRNAs mis-spliced in diabetic hearts.

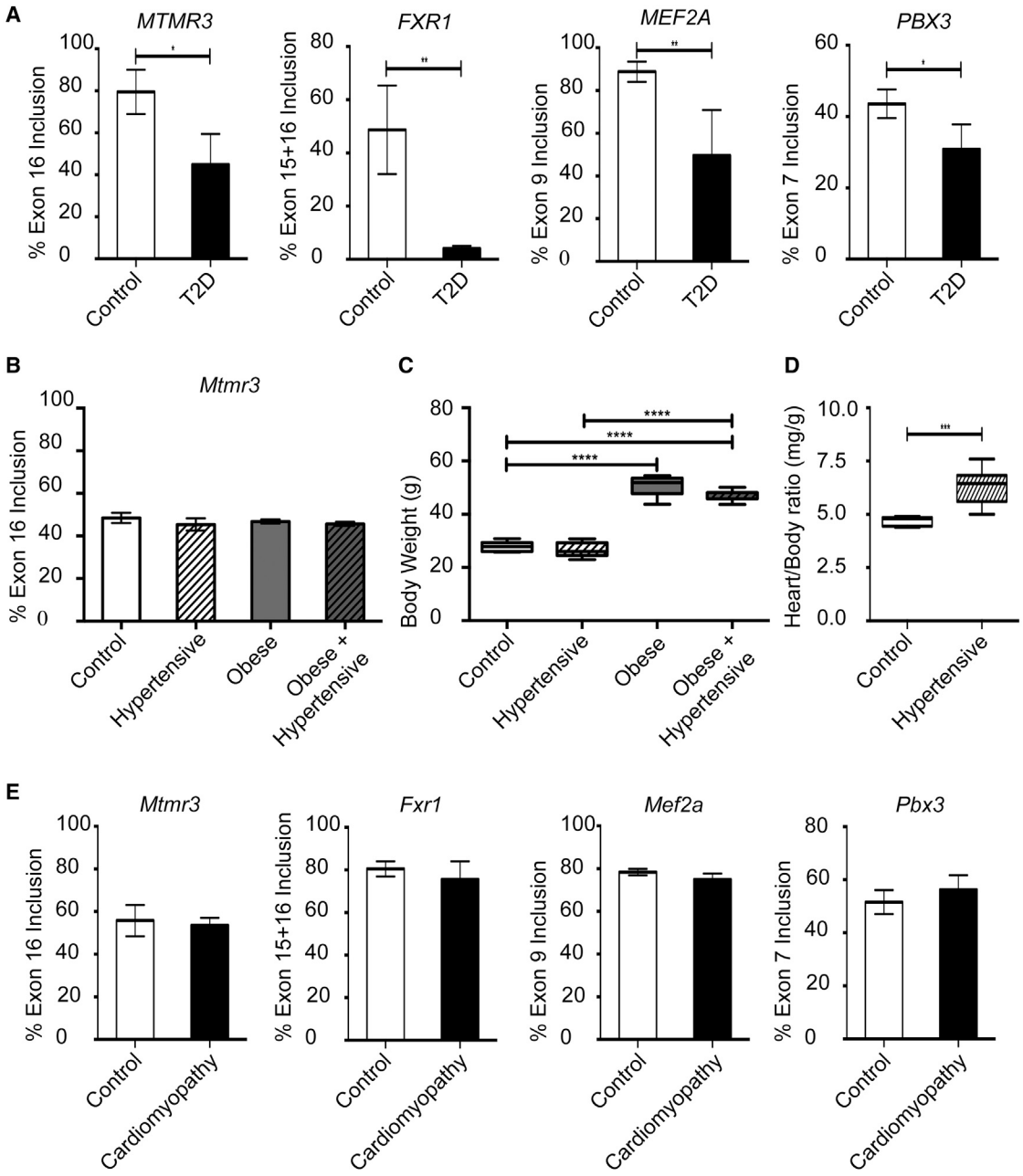

Figure 2. AS of RBFOX2 Targets Is Disrupted in Diabetic Hearts Independent of Hypertension and Obesity

(A) Percent inclusion of *MTMR3* exon 16, *FXR1* exon 15+16, *MEF2A* exon 9, and *PBX3* exon 7 as determined by qRT-PCR in non-diabetic (control) or type 2 diabetic (T2D) human left ventricles (n ≥ 3).

(B) AS analysis of *Mtmr3* exon 16 in hypertensive, obese, and obese-hypertensive mouse models (see also Figure S2; n = 3).

(C) Body weight of mock-treated control, angiotensin-II-treated hypertensive, obese, and angiotensin-II-treated obese mice.

(D) Heart-to-body-weight ratio of mock-treated control mice or angiotensin-II-treated hypertensive mice.

(E) AS analysis in chagasic mice with severe cardiomyopathy and heart failure. *Mtmr3* exon 16, *Fxr1* exon 15+16, *Mef2a* exon 9, and *Pbx3* exon 7 AS was determined in non-infected (control) or chronically infected chagasic mice with cardiomyopathy (cardiomyopathy; n ≥ 3).

Data represent means ± SD. Statistical significance was calculated using unpaired t test for two group comparisons or using one-way ANOVA to compare four different groups. p values are represented as **** < 0.0001, *** < 0.001, ** < 0.01, and * < 0.05.

To further investigate whether decreased RBFOX2 levels induce the AS patterns of diabetic hearts, we performed RBFOX2 depletion studies in rat-heart-derived cells (H9c2) and tested endogenous AS events dysregulated in diabetic hearts. We used both small interfering RNA (siRNA) and small hairpin RNA (shRNA) to target different regions of *Rbfox2* (Figure 3A).

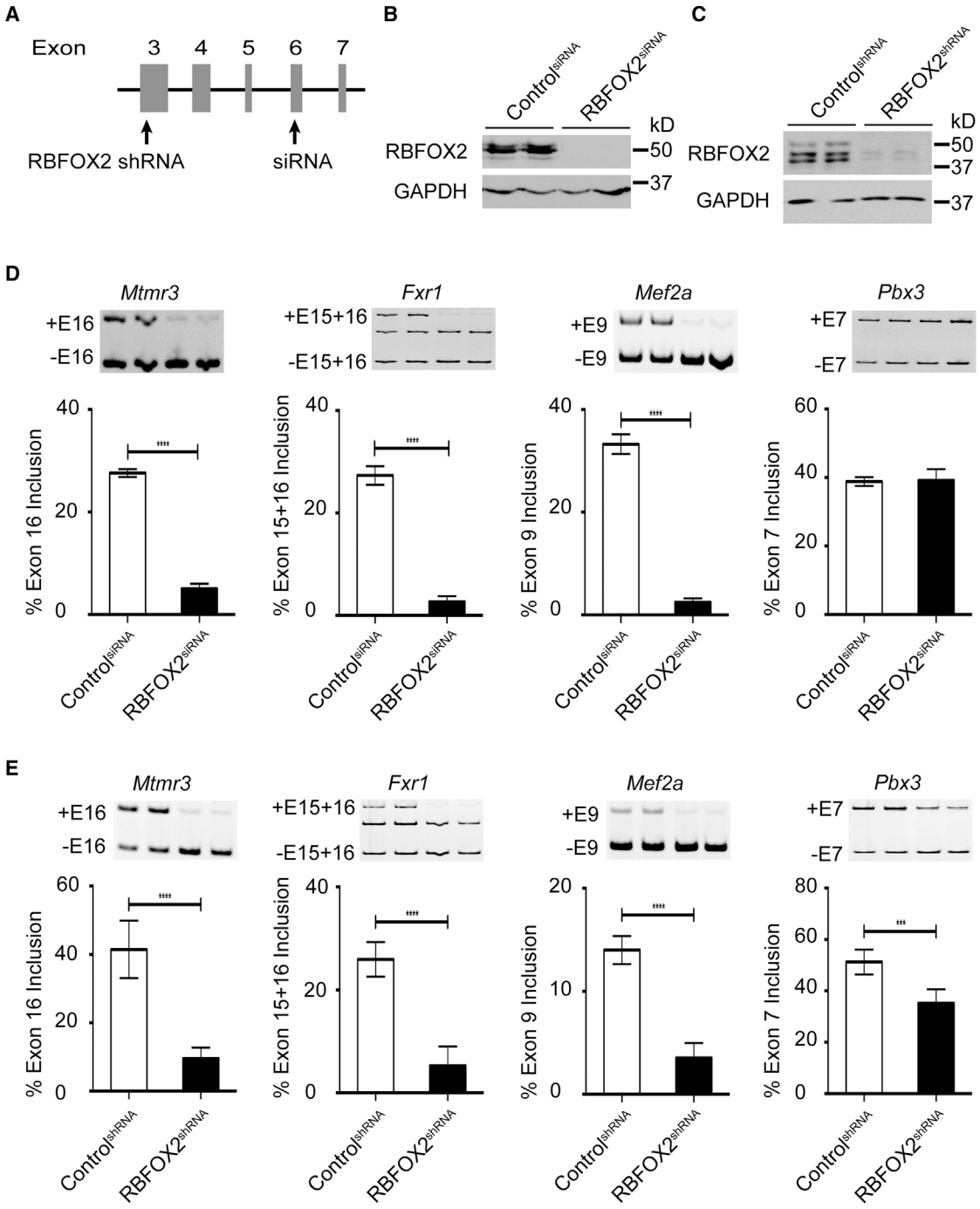

Figure 3. RBFOX2 Regulates AS Events Altered in Diabetic Hearts

(A) Schematic of *Rbfox2* pre-mRNA (only exons 3–7) regions targeted by siRNA and shRNA. Introns were not drawn to scale.

(B) Total protein lysates from siRNA-treated H9c2 cells analyzed by western blotting (WB) using an antibody (Ab) against RBFOX2 to determine the depletion efficiency of *Rbfox2* siRNA. GAPDH WB was performed to confirm even protein loading.

(C) RBFOX2 protein levels determined in shRNA-expressing H9c2 cells by WB using an anti-RBFOX2 Ab. GAPDH WB was used as a loading control.

(D) AS analysis of *Mtmr3* exon 16, *Fxr1* exon 15+16, *Mef2a* exon 9, and *Pbx3* exon 7 in H9c2 cells transfected with scrambled (control) or *Rbfox2*-specific siRNA (targets exon 6; $n \geq 8$).

(E) AS analysis in H9c2 cells transfected with scrambled (control) or *Rbfox2*-specific shRNA (targets exon 3; $n \geq 6$).

In AS gel figures, +E# is exon no. inclusion and −E# is exon no. exclusion. Data represent the means ± SD. The unpaired t test was used to calculate statistically significant differences between two sample groups from three independent experiments. p values are indicated as **** < 0.0001 and *** < 0.001.

Please cite this article in press as: Nutter et al., Dysregulation of RBFOX2 Is an Early Event in Cardiac Pathogenesis of Diabetes, Cell Reports (2016), http://dx.doi.org/10.1016/j.celrep.2016.05.002

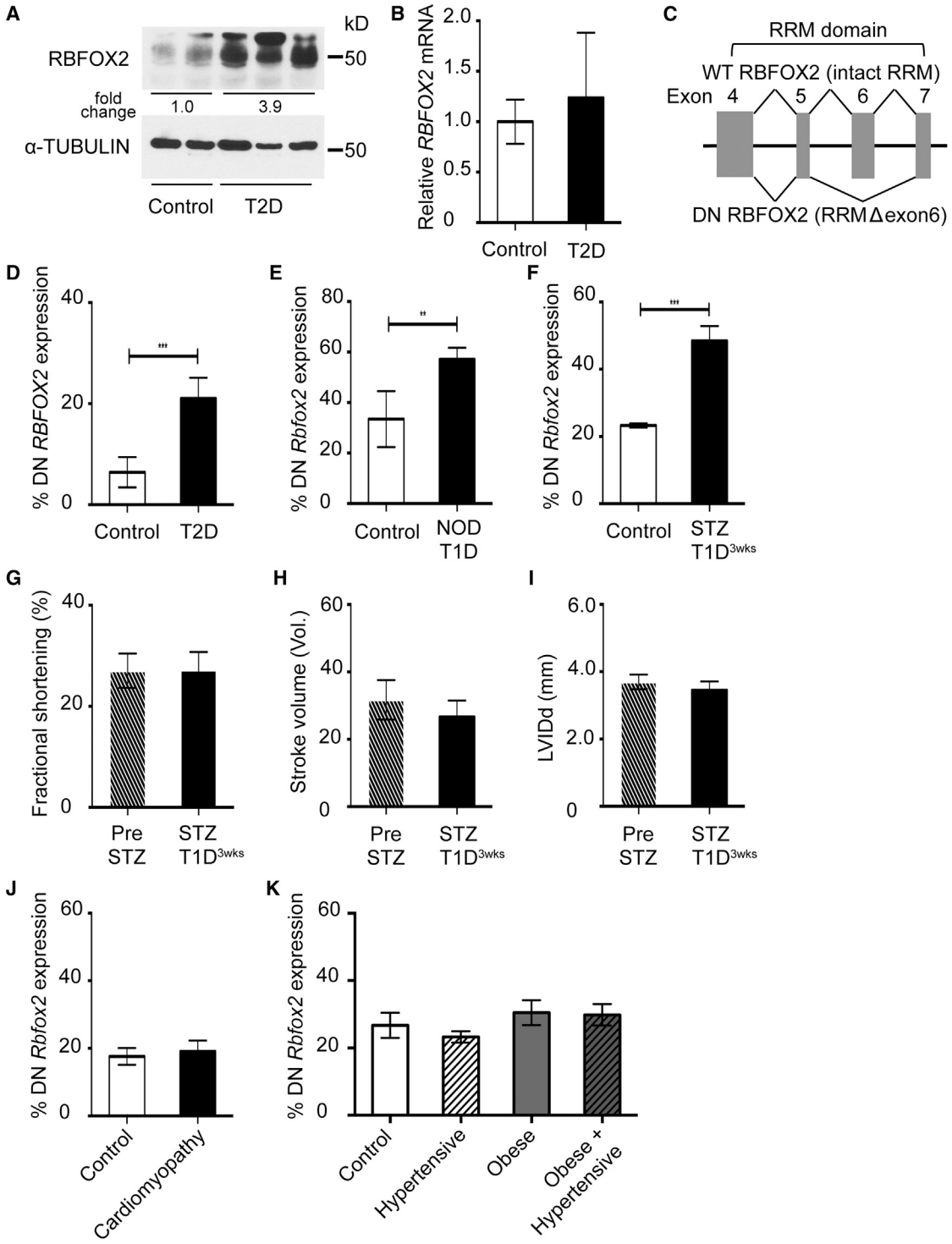

Figure 4. DN *RBFOX2* Is Generated in Diabetic Hearts at Early Stages

(A) WB analysis of RBFOX2 protein in non-diabetic control or T2D human left ventricles using an anti-RBFOX2 Ab. α-TUBULIN WB was used as a loading control. Fold change in RBFOX2 protein levels was determined after normalizing protein levels to α-TUBULIN, the control averages were set to 1, and patient averages were summarized below.

(B) Relative *RBFOX2* mRNA levels in non-diabetic control and T2D human patients' hearts, determined by qRT-PCR ($n \geq 5$).

(C) Schematic of DN *RBFOX2* generation via exon 6 exclusion (RRM, RNA recognition motif). Introns were not drawn to scale.

(legend continued on next page)

Alternative exons with RBFOX2-binding sites (*Mtmr3* exon 16, *Fxr1* exon 15+16, and *Mef2a* exon 9; Figure 1E) had less exon inclusion in RBFOX2-depleted cells (Figures 3B and 3D), similar to that in diabetic hearts (Figure 3D versus Figure 2A). As an additional control, we depleted RBFOX2 using an shRNA targeting a different region in the *Rbfox2* mRNA (exon 3; Figures 3A and 3C) to make sure that changes in AS were due to specific depletion of RBFOX2. Cells expressing *Rbfox2*-specific shRNA displayed AS patterns similar to those in *Rbfox2* siRNA-treated cells (Figure 3E versus Figure 3D) and in T2D human patients' hearts (Figure 2A), indicating that low RBFOX2 levels or activity trigger the AS patterns of diabetes. AS of *Pbx3* was unaffected in *Rbfox2* siRNA-treated cells (Figure 3D), consistent with its lack of RBFOX2-binding sites (Figure 1E), but was affected in *Rbfox2* shRNA-treated cells (Figure 3E). It is possible that *PBX3* could be an indirect downstream target of RBFOX2 because its AS was altered only after prolonged shRNA treatment. These results show that pre-mRNAs with RBFOX2-binding sites are differentially spliced in T2D human hearts, consistent with low RBFOX2-dependent splicing.

High RBFOX2 Protein Levels in Diabetic Hearts Are Consistent with Increased Expression of a DN Isoform of *RBFOX2*

We have previously shown that RBFOX2 protein levels are elevated in T1D mouse hearts (Verma et al., 2013), which is contradictory to our new findings of low RBFOX2 AS activity in diabetic hearts. We thought that RBFOX2 might be regulated differently in T2D versus T1D. Therefore, we tested RBFOX2 protein levels in T2D human patients' hearts. Consistent with our data in T1D mice, RBFOX2 protein levels were also elevated in T2D patients' hearts (Verma et al., 2013; Figure 4A). To determine whether the increase in RBFOX2 protein levels was due to increased mRNA levels, we performed qRT-PCR using *RBFOX2*-specific primers in T2D patients' hearts and age-matched non-diabetic controls. There was no significant increase in *RBFOX2* mRNA levels in diabetic hearts (Figure 4B) that could explain high protein levels (Figure 4A), suggesting that RBFOX2 protein levels are regulated post-transcriptionally.

To better understand how RBFOX2 is dysregulated in diabetic hearts, we examined the expression of a DN *RBFOX2* isoform that is capable of repressing the AS activity of RBFOX family of proteins (including RBFOX1, RBFOX2, and RBFOX3; Damianov and Black, 2010; Nakahata and Kawamoto, 2005). DN RBFOX2 is generated via exclusion of exon 6, which encodes half of the RNA recognition motif (RRM), resulting in low RNA-binding capability and newly gained RBFOX repressor activity (Damianov and Black, 2010; Nakahata and Kawamoto, 2005; Figure 4C). We found that the DN *RBFOX2* isoform lacking exon 6 was increased in both T1D mouse models (non-obese diabetic [NOD] and streptozotocin [STZ] induced) as well as in T2D human patients' hearts (Figures 4D–4F). To determine whether expression of DN *Rbfox2* is an early event in diabetic cardiomyopathy, we examined cardiac function before and after induction of diabetes by STZ using echocardiography. Left ventricle (LV) function, stroke volume, and ventricular internal diameter end at diastole (LVIDd) were unaffected after 3 weeks of hyperglycemia (Figures 4G–4I). These results show that DN *Rbfox2* upregulation and changes in AS of RBFOX2 targets occurred before cardiac complications were detectable in diabetic mice, indicating that DN *Rbfox2* expression is an early response to high glucose levels. We also examined DN *Rbfox2* expression in other mouse models. DN *Rbfox2* mRNA levels were not increased in hypertensive, obese, obese-hypertensive, or mice with cardiomyopathy when compared to controls (Figures 4J and 4K). Consistent with these mouse models' lack of increase in DN *Rbfox2* expression, AS patterns of RBFOX2 targets were also unaffected (Figures 4J and 4K versus Figures 2B, 2E, and S2). These results show that the DN version of *RBFOX2* is generated in both T1D mouse and T2D patients' hearts as an early event, and the expression of DN *RBFOX2* is consistent with aberrant AS of RBFOX2 targets in diabetic hearts.

Increased RBFOX2 Protein Levels with RNA-binding Capability Induce DN *Rbfox2* Expression

We investigated how DN *RBFOX2* is generated in diabetic hearts. RBFOX2 AS activity is controlled such that an increase in RBFOX2 protein levels leads to expression of the DN version via autoregulation of exon 6 exclusion (Damianov and Black, 2010). We tested whether DN *Rbfox2* is generated due to high levels of RBFOX2 and whether RNA-binding activity of RBFOX2 is required. We expressed RBFOX2 in H9c2 cells and examined endogenous DN *Rbfox2* expression by qRT-PCR. As a control, an RNA-binding-deficient mutant of RBFOX2 ($RBFOX2^{RRM}$) was expressed. $RBFOX2^{RRM}$ mutant lacks RNA-binding activity due to mutagenesis of two critical phenylalanine residues in the RRM necessary for RNA-binding (Auweter et al., 2006; Mayeda et al., 1994; Sun et al., 2012). We found that overexpression of $RBFOX2^{WT}$ (Figure 5A) capable of binding to RNA increased the expression of the DN *Rbfox2* isoform (Figure 5B). However, $RBFOX2^{RRM}$ mutant (Figure 5A) did not affect DN expression as robustly as the WT (Figure 5B), demonstrating that the RNA-binding function of RBFOX2 is critical for autoregulation and DN *Rbfox2* generation.

(D) DN *RBFOX2* mRNA levels were determined by *RBFOX2* exon 6 exclusion using qRT-PCR from left ventricles of T2D human patients or non-diabetic controls ($n \geq 5$).
(E) DN *Rbfox2* expression in hearts from non-diabetic control mice or non-obese diabetic (NOD:T1D) mice ($n \geq 4$).
(F) DN *Rbfox2* expression in hearts from mock-injected control or streptozotocin-induced T1D ($STZ:T1D^{3wks}$) mice hyperglycemic for 3 weeks ($n \geq 3$).
(G–I) Cardiac function of mice before (pre-STZ) or 3 weeks after hyperglycemia ($STZ:T1D^{3wks}$) was assessed by M-mode echocardiography measuring (G) fractional shortening (%), (H) stroke volume (vol.), and (I) ventricular internal diameter end at diastole (LVIDd) (mm; $n \geq 3$).
(J) DN *Rbfox2* expression in left ventricles from chagasic mice with severe cardiomyopathy or mock-infected controls ($n \geq 3$).
(K) DN *Rbfox2* expression pattern in left ventricles of obese, hypertensive, and obese-hypertensive mouse left ventricles ($n = 3$).
Data represent the means ± SD. Statistical significance between two groups was calculated using the unpaired t test and between four groups using one-way ANOVA. p values are indicated as *** < 0.001 and ** < 0.01.

Please cite this article in press as: Nutter et al., Dysregulation of RBFOX2 Is an Early Event in Cardiac Pathogenesis of Diabetes, Cell Reports (2016), http://dx.doi.org/10.1016/j.celrep.2016.05.002

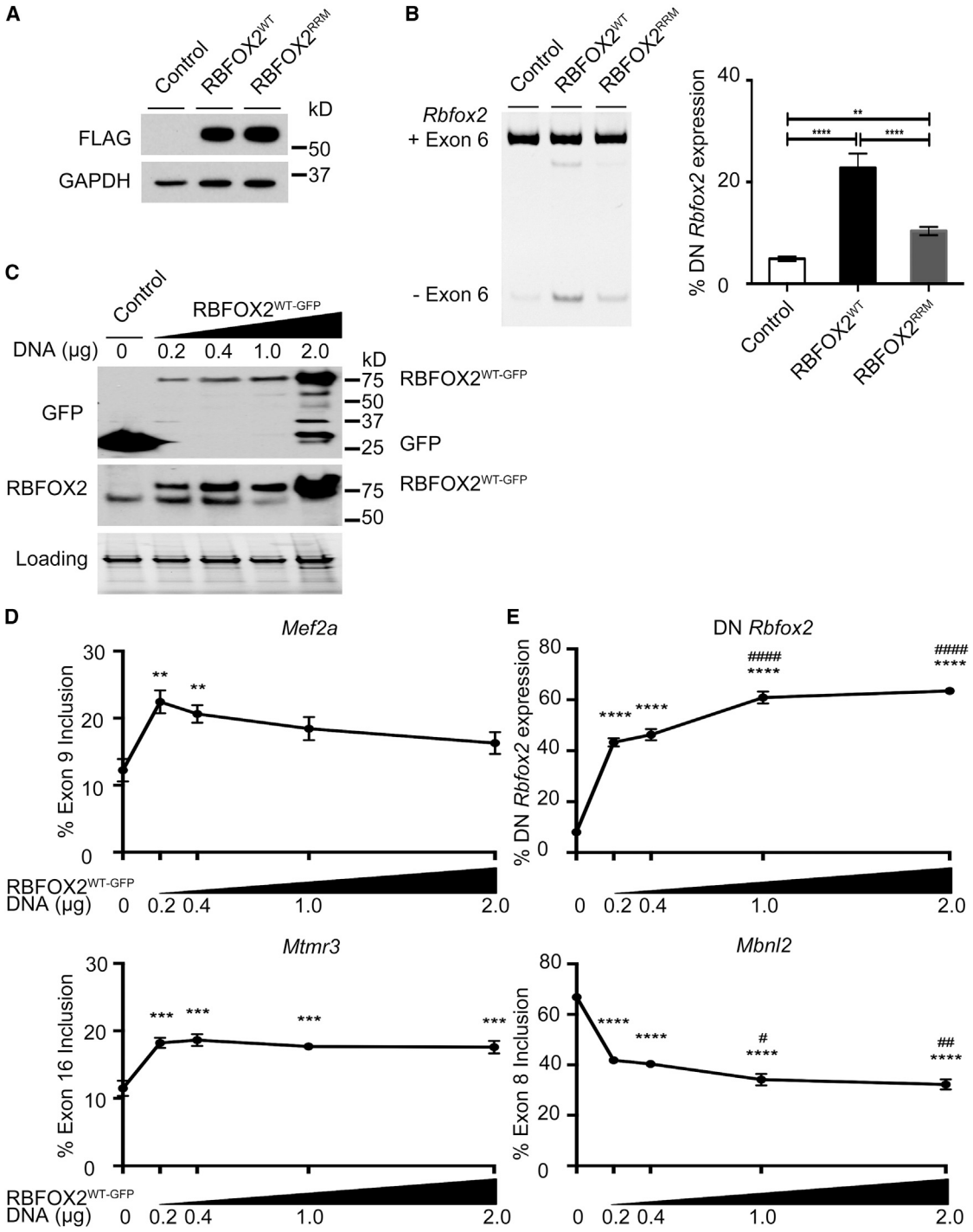

Figure 5. Increased RBFOX2 Protein with RNA-binding Capability Is Important for Generation of DN *Rbfox2*

(A) WB analysis of RBFOX2 in H9c2 cells expressing empty vector (control), RBFOX2^{WT}, or RBFOX2^{RRM} (RNA-binding-deficient mutant).

(B) Endogenous DN *Rbfox2* expression by exclusion of exon 6 in H9c2 cells expressing control, RBFOX2^{WT}, or RBFOX2^{RRM} determined by qRT-PCR (n = 4 from three independent experiments). Data represent the means ± SD.

(C) RBFOX2 WB in H9c2 cells expressing GFP or increasing levels of GFP-tagged RBFOX2 using anti-GFP or anti-RBFOX2 Ab. Ponceau S staining was used to assess even protein loading.

(legend continued on next page)

Next, we examined whether there is a threshold for RBFOX2 protein levels to have an inhibitory splicing effect by generating DN RBFOX2. To test this, we performed a dose response experiment by expressing increasing concentrations of GFP-RBFOX2 but keeping total transfected DNA concentration the same and tested AS of RBFOX2 targets. Expression levels of endogenous DN *Rbfox2* were also monitored. As a negative control, we used GFP. Figure 5C shows an exponential increase in GFP-RBFOX2 protein levels determined by western blot (WB) using both GFP and RBFOX2 antibodies. At the lowest dose of WT RBFOX2, all four exons targeted by RBFOX2 were affected such that Mef2a, Mtmr3, and Fxr1 alternative exons were more included (Figures 5D and S3). However, as the RBFOX2 dose increased, *Mef2a* exon 6 inclusion was inhibited (Figure 5D) and exon inclusions of *Mtmr3* and *Fxr1* were not further increased, coincident with upregulation of endogenous DN *Rbfox2* (Figure 5E). Because the endogenous *Rbfox2* pre-mRNA level is the limiting factor in generation of DN RBFOX2 in response to high levels of WT RBFOX2, it is possible that only exons very sensitive to changes in RBFOX2 were inhibited and others were prevented at high WT RBFOX2 doses. On the contrary, exon 6 exclusion of *Rbfox2* was not inhibited at any concentration of WT RBFOX2 (Figure 5E) that adversely affected exon inclusions (Figures 5D and S3). Indeed, *Rbfox2* exon 6 was excluded continuously from 92% to 36% as the WT RBFOX2 concentrations increased, suggesting that WT RBFOX2 was not effective in inhibiting exon 6 exclusion; thus, DN *Rbfox2* generation (Figure 5E). To test whether WT RBFOX2 overexpression has any effect on other exon exclusion events, we analyzed *Mbnl2* exon 8. At low WT RBFOX2 dose, *Mbnl2* exon 8 inclusion decreased from 67% to 42% (Figure 5E). At higher doses of WT RBFOX2, *Mbnl2* exon 8 was 10% further excluded down to 32% (Figure 5E). Whereas *Mbnl2* and *Rbfox2* exons continued to be excluded as WT RBFOX2 concentration increased, exon inclusion events were either inhibited or prevented. These results suggest that overexpression of WT RBFOX2 may be ineffective in inhibiting exon exclusion. Overall, aberrant upregulation of RBFOX2 above a threshold becomes ineffective or even inhibitory in regulating RBFOX2-dependent exon inclusion.

Increased RBFOX2 Protein Levels during Myocardial Differentiation Correlates with Upregulation of DN *Rbfox2*

RBFOX2 protein levels are dynamically regulated during cardiomyocyte differentiation (Verma et al., 2013). To further test whether high RBFOX2 protein levels are responsible for DN *Rbfox2* induction, we examined DN *Rbfox2* expression during cardiomyocyte differentiation. Successful differentiation was confirmed by upregulation of cardiac troponin T (cTNT) using WB (Figure S4A). In differentiated cells, RBFOX2 protein levels were elevated by 3.6-fold, corresponding to a 40% increase in DN *Rbfox2* expression when compared to undifferentiated cells (Figures S4A and S4B). These results support our findings that, when RBFOX2 levels increase over a threshold, it induces DN expression (Figures 4, 5, and S4).

DN RBFOX2 Interacts with WT RBFOX2 and Inhibits AS of RBFOX2 Targets

The next important question was to determine whether ectopic expression of DN RBFOX2 inhibits AS similar to that observed in diabetic hearts. For that reason, we expressed FLAG-DN RBFOX2 in H9c2 cells (Figure 6A) and tested AS of RBFOX2-responsive targets. FLAG-DN RBFOX2 expression induced exon exclusion of targets (Figure 6B) resembling AS patterns in diabetic hearts (Figure 6B versus Figure 2A). This result indicates that the DN *RBFOX2* upregulation in diabetic hearts impairs RBFOX2-dependent splicing.

To investigate whether DN RBFOX2 inhibits splicing via sequestering spliceosome components known to interact with RBFOX2, we overexpressed either FLAG-tagged WT or DN RBFOX2 in COS M6 cells and performed FLAG immunoprecipitation (IP) to assess the binding of RBFOX2 to U1 snRNP. It was previously shown that RBFOX2 binds to U1C to assemble the U1 small nuclear ribonucleoprotein particle (snRNP) complex and promote splicing (Huang et al., 2012). We also tested whether the RNA-binding-deficient mutant of RBFOX2 ($RBFOX2^{RRM}$) can interact with U1C. To determine whether there is non-specific protein binding to the FLAG-antibody-coated beads, we used protein lysates from cells expressing empty vector (control). Loading control shows equal amounts of lysates (input) loaded onto beads coated with similar amounts of FLAG-antibody (immunoglobulin G [IgG]; Figures 6C and 6D). As expected, WT RBFOX2 pulled down endogenous U1C protein (Figure 6C). However, neither $RBFOX2^{RRM}$ nor DN RBFOX2 was able to pull down U1C (Figure 6C), indicating that RBFOX2 mutants lacking RNA-binding activity do not interact with U1C. DN proteins are known to bind to the WT protein counterpart to inhibit activity. To test whether DN RBFOX2 interacts with WT RBFOX2 to inhibit its splicing activity, we co-expressed GFP-WT RBFOX2 with FLAG-DN RBFOX2 and performed FLAG-IP. GFP-WT RBFOX2 was pulled down together with FLAG-DN RBFOX2, indicating that DN and WT RBFOX2 proteins interact (Figure 6D). These results suggest that DN RBFOX2 inhibits AS via interacting with WT RBFOX2 not by sequestering U1C.

Dysregulation of RBFOX2 Adversely Affects Cytoskeleton-Associated Gene Function and Intracellular Calcium Handling

To determine the consequences of RBFOX2-induced AS defects, we focused on the downstream targets of RBFOX2. Ablation of the RBFOX2 target gene *Fxr1* in animal models causes cardiomyopathy, partly by upregulation of the TALIN2 protein,

(D and E) AS of (D) *Mef2a* and *Mtmr3* and (E) *Mbnl2* and expression levels of DN *Rbfox2* in H9c2 cells expressing increasing levels of $RBFOX2^{WT-GFP}$ (see also Figure S3). To equalize the amount of DNA per plate to 2 μg, different concentrations of vector DNA were transfected together with $RBFOX2^{WT-GFP}$. Quantifications were performed using samples from at least four independent experiments ($n \geq 4$).

Data represent the means ± SE. Statistical significance was calculated using one-way ANOVA to compare three or more different groups. p values are indicated as **** < 0.0001, *** < 0.001, and ** < 0.01 compared to the GFP control (0 μg RBFOX2 DNA). p values indicated as #### < 0.0001 represent comparisons to the lowest $RBFOX2^{WT-GFP}$ level (0.2 μg RBFOX2 DNA).

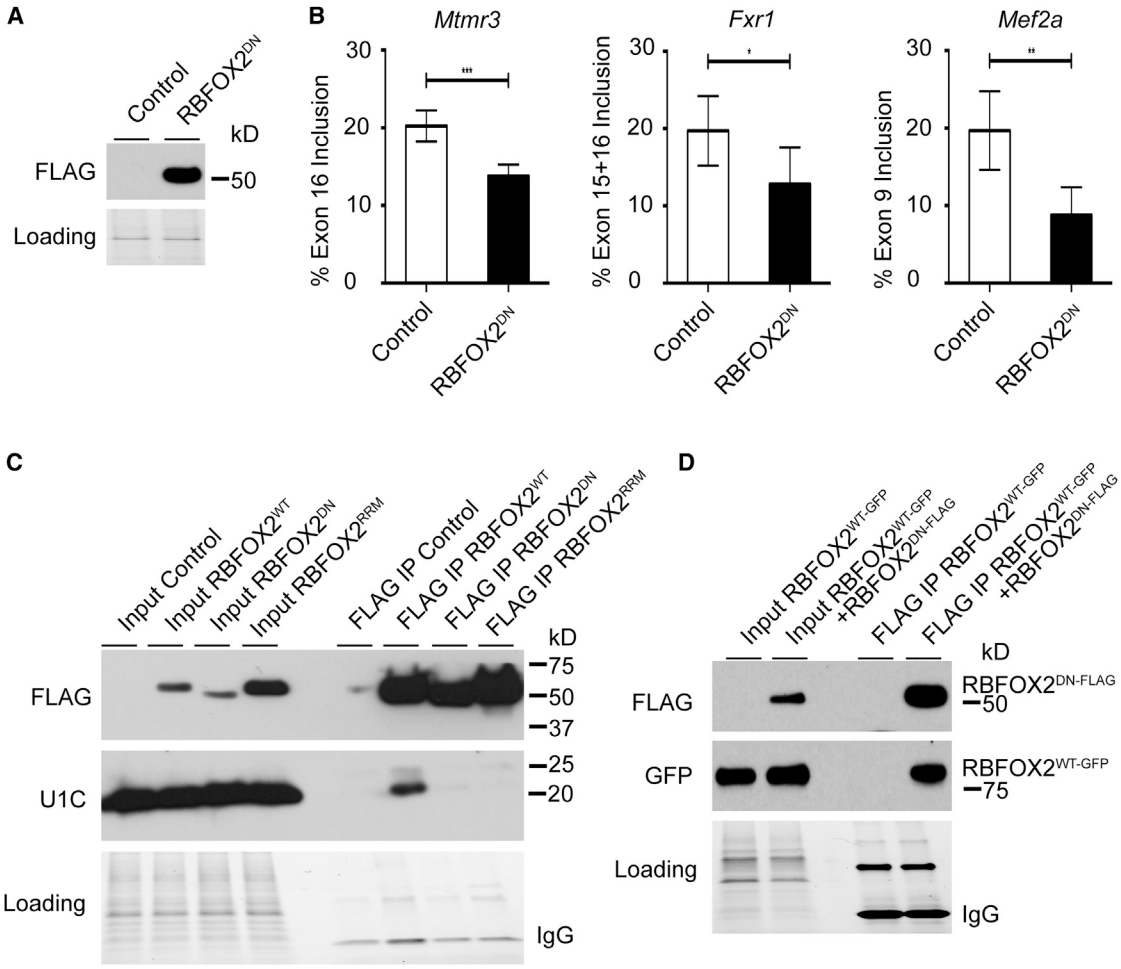

Figure 6. DN RBFOX2 Interacts with WT RBFOX2 and Inhibits AS of RBFOX2-Regulated Splicing

(A) WB analysis of DN RBFOX2 protein in H9c2 cells expressing empty vector (control) or FLAG-RBFOX2^{DN}.

(B) AS analysis of *Mtmr3*, *Fxr1*, and *Mef2a* in H9c2 cells transfected with empty vector (control) or FLAG-RBFOX2^{DN} ($n \geq 4$).

(C) Interactions of FLAG-tagged RBFOX2^{WT}, RBFOX2^{DN}, and RBFOX2^{RRM} (RNA-binding-deficient mutant) with U1C protein in COS M6 cells determined by FLAG IP followed by WB using FLAG and U1C-specific Abs.

(D) Interactions of FLAG-RBFOX2^{DN} with GFP-RBFOX2^{WT} in H9c2 cells. Pulled-down proteins were analyzed by WB using HRP-conjugated anti-FLAG and anti-GFP Abs. Control lysates expressing empty vector were used as a negative control for non-specific protein binding to the FLAG-antibody-coated beads (FLAG-IP control). Input lysates represent 1/20 of total protein loaded onto the FLAG beads. Results are representative of three independent experiments.

which functions in the assembly of the actin cytoskeleton (Whitman et al., 2011). *FXR1* exons 15 and 16, necessary for striated muscle-specific translational regulation (Kirkpatrick et al., 1999), are almost completely excluded in diabetic human hearts (Figure 2A) and in RBFOX2-depleted cells (Figures 3D and 3E). When we checked TALIN2 protein levels in RBFOX2-depleted cells, TALIN2 protein levels were significantly elevated (Figure 7A). TALIN2 protein levels were also upregulated in T1D mouse hearts (Figure 7B). This result shows that low RBFOX2 levels/activity correlates with increased TALIN2 protein levels in diabetic mouse hearts.

Next, we tested whether DN RBFOX2 expression affects cardiomyocyte function. It has been previously shown that ablation of *Rbfox2* in adult mouse hearts impairs excitation:coupling (Wei et al., 2015), and our results show that RBFOX2 targets affected in diabetic hearts have functions in calcium homeostasis (Figure 1C). Thus, we examined intracellular calcium handling in human cardiomyocytes expressing DN RBFOX2. DN RBFOX2 expression induced a delayed upstroke of the calcium transients in cardiomyocytes (Figures 7C and 7D) without a change in calcium transient amplitudes (Figure 7E), indicating a defect in intracellular calcium handling, which is necessary for cardiomyocyte contraction. In sum, our results show that DN RBFOX2 may contribute to diabetes pathogenesis by altering intracellular calcium signaling.

DISCUSSION

We have previously shown that AS is dysregulated in diabetic hearts. Our goal in this study was to determine the responsible

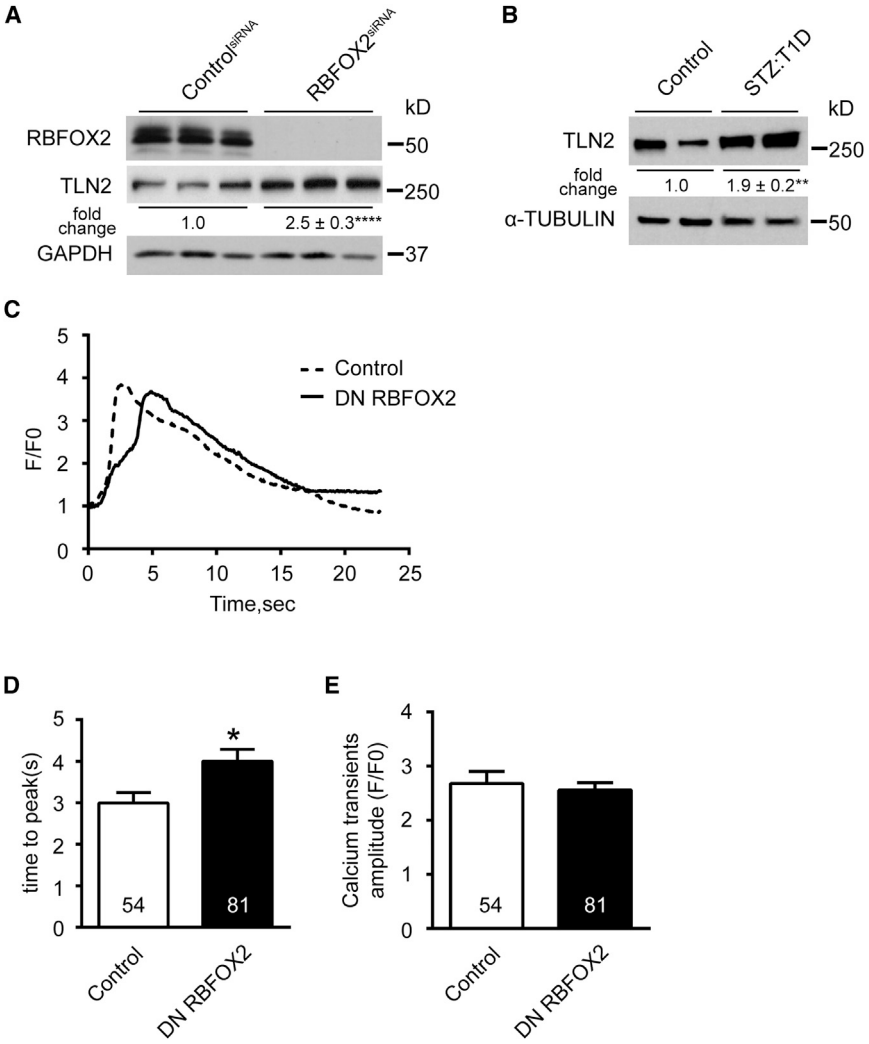

Figure 7. Consequences of Aberrant AS of RBFOX2 Targets

(A) WB analysis of TALIN2 (TLN2), RBFOX2, and GAPDH in H9c2 cells treated with scrambled siRNA (control) or *Rbfox2*-specific siRNA. Fold changes in TLN2 protein levels were determined after normalizing to GAPDH protein levels ($n \geq 9$ from three independent experiments).

(B) Representative WB analysis of TLN2 protein levels in STZ:T1D mice. α-TUBULIN WB was used as a loading control. Fold changes in TLN2 levels were determined after quantifying protein levels and normalizing to α-TUBULIN levels. TLN2 levels in control mice were set as 1. Average values were represented as means ± SD (n = 4).

(C) Representative tracing of calcium transients from human primary cardiomyocytes infected with AAV9-CMV-null (control) and AAV9-CMV-DN RBFOX2 (DN RBFOX2).

(D and E) Quantification of (D) time to peak and (E) amplitude of calcium transients. The numbers in the bar graphs represent the number of cardiomyocytes used for quantification from three independent experiments.

Statistical significance was calculated using the unpaired t test to compare two groups. p values are indicated as **** < 0.0001, ** < 0.01, and * < 0.05.

AS regulators. We found that the RNA-binding protein RBFOX2 contributes to AS defects in the heart under diabetic conditions. Comparing our RNA sequencing data from diabetic mouse hearts to the RBFOX2 CLIP-seq data (NCBI: SRP030031 and SRP029987), we found that RBFOX2 binds to 73% of transcripts that are differentially spliced. In diabetic hearts, RBFOX2-binding clusters were significantly enriched in mis-spliced transcripts in comparison to control transcripts that were not mis-spliced but displayed similar expression levels. Importantly, we found that RBFOX2 controls AS of target genes with RBFOX2-binding sites and that AS changes impair normal gene expression patterns in the heart, especially genes important for macromolecular metabolism, apoptosis, calcium homeostasis, and protein trafficking. Supporting these findings, expression of DN RBFOX2 in cardiomyocytes impaired intracellular calcium handling.

We found that RBFOX2 autoregulation is disrupted in diabetic hearts at early stages before cardiac complications are evident. RBFOX2-mediated splicing function was low in diabetic hearts due to the expression of the DN *RBFOX2*. A recent study has shown that heart-specific deletion of *Rbfox2* in mice induces dilated cardiomyopathy (Wei et al., 2015). Our results demonstrate that expression of DN RBFOX2, which inhibits RBFOX2-dependent splicing, adversely affects calcium handling in human cardiomyocytes. These results support the conclusion that increased DN *RBFOX2* expression in diabetic hearts contributes to cardiac complications.

In this study, we discovered that a DN isoform of *RBFOX2* is upregulated in hearts of both human diabetic patients and mouse models via skipping of exon 6 induced by an increase in RBFOX2 protein levels. This isoform was identified as an inhibitor of RBFOX AS activity in cultured cells (Damianov and Black, 2010; Nakahata and Kawamoto, 2005). *RBFOX2* has consensus binding sites in the flanking introns of exon 6, which is skipped in the DN isoform (Damianov and Black, 2010). Here, we showed that increased RBFOX2 protein in diabetes is important for DN *RBFOX2* production in diabetic hearts and found that RBFOX2 RNA-binding capability is critical for generation of DN *RBFOX2* via AS. Therefore, it is likely that RBFOX2 binds to its own pre-mRNA to promote exon 6 exclusion and DN expression.

An important part of our finding is that the dysregulation of AS in diabetic hearts is in agreement with the upregulation of DN *RBFOX2*. Notably, RBFOX2 target AS events were unaffected in obese and hypertensive mice that do not upregulate DN *Rbfox2*. We also found that RBFOX2-regulated AS events remained unchanged in mouse hearts with chagasic cardiomyopathy in which DN *Rbfox2* expression is not induced.

Please cite this article in press as: Nutter et al., Dysregulation of RBFOX2 Is an Early Event in Cardiac Pathogenesis of Diabetes, Cell Reports (2016), http://dx.doi.org/10.1016/j.celrep.2016.05.002

These results indicate that the expression of DN *RBFOX2* is stimulated under diabetic conditions independent of hypertension and obesity. In addition, DN RBFOX2 overexpression impaired AS of RBFOX2 targets. Here, we provide strong evidence for mode of inhibitory function of DN RBFOX2 on RBFOX2-dependent splicing by finding that DN RBFOX2 interacts with WT RBFOX2 but does not interact with the U1snRNP-associated U1C.

In our study, *FXR1* exons 15 and 16 were almost completely skipped in diabetic human hearts. FXR1 regulates mRNA translation of *TALIN2*, an important regulator of actin assembly (Whitman et al., 2011). FXR1 knockout mice develop cardiomyopathy in part due to increased translation and accumulation of TALIN2 (Whitman et al., 2011). Our data indicate that RBFOX2 knockdown results in exclusion of *Fxr1* exon 15 and 16 and, in turn, high TALIN2 levels similar to the levels observed in diabetic hearts. These results suggest a role for RBFOX2 in regulating cytoskeleton-interacting protein contributing to diabetic cardiomyopathy.

In summary, we find that 704 alternative exons mis-spliced in diabetic hearts are RBFOX2 targets. RBFOX2 protein levels go up in diabetic hearts, inducing an AS change in *RBFOX2* pre-mRNA that generates a DN isoform with inhibitory AS function, contributing to AS changes with adverse effects on gene expression and function. Importantly, DN *RBFOX2* is generated specifically in diabetic hearts at early stages, making it a potential diagnostic marker for diabetic cardiomyopathy. Identifying RBFOX2 as an important contributor to AS changes and diabetic complications and determining how it is dysregulated may allow us to develop novel tools to diagnose, prevent, or treat diabetic cardiomyopathy in the future.

EXPERIMENTAL PROCEDURES

Animal Experiments

Animal models used for this study are as follows: STZ-induced T1D and NOD, obese, hypertensive, obese-hypertensive, and chagasic mice. Details about these mouse models are found in the 16-00055 Supplemental Experimental Procedures.

All animal experiments were conducted in accordance with the NIH guidelines and approved by the University of Texas Medical Branch Institutional Animal Care and Use Committee (protocol no. 1101001).

Echocardiography

Cardiac function was assessed using M-mode echocardiography with a Visual Sonics VeVo 2100 ultrasound and a 30 MHz probe at the UTMB Biomedical Imaging Network. Mice were anesthetized (1.5% isoflurane mixed with 95% oxygen) and maintained on a heated platform with echocardiogram (ECG) electrodes to measure body heat and heart rate before and during the imaging. Mice with a heart rate of 450 ± 50 and body temperature of at least 37°C were used for all analyses. Fractional shortening, stroke volume, and LVIDd were calculated as described previously (Liu et al., 2012) using Visual Sonics software at the Baylor College of Medicine Mouse Phenotyping Core.

Human Tissue

Human heart tissues (diabetic and non-diabetic) were obtained from the National Disease Research Interchange. Two additional non-diabetic human heart tissues were obtained from Dr. Nisha Garg at the University of Texas Medical Branch. All human heart tissues used in this study were pre-existing and deidentified. Thus, human tissue use was exempt from Institute Review Board regulations (protocol no. 11-087).

Cell Culture, Differentiation, and Transfections

Cells were cultured and transfected using standard procedures as previously described (Verma et al., 2013). H9c2 cells were differentiated into cardiomyocyte-like cells as described previously (Verma et al., 2013). Human Prenatal Primary Cardiomyocytes (DV Biologics) were cultured according to the manufacturer's protocols and infected with AAV9 virus (Vector Biolabs) to express either empty vector or DN RBFOX2. Details are found in the Supplemental Experimental Procedures.

Calcium Imaging

For calcium imaging, human primary cardiomyocytes (DV Biologics) were incubated at 20°C with 8 μM calcium indicator Fluo-4-AM (Life Technologies; F14201) for 10 min and imaged in Hank's balanced salt solution (pH 7.4) using an Olympus IX51 microscope (20×) and CelSens Standard version 1.4.1 software.

RNA Sequencing, RBFOX2-binding Site Overlay, and Statistical Analysis

An Illumina HiSeq 1000 system was used for paired end (2 × 15 cycles) RNA sequencing at the UTMB Next-Generation Sequencing Core facility (Verma et al., 2013). Approximately 200 million reads per sample were generated. Changes in AS were determined using the mixture-of-isoforms (MISO) model (Katz et al., 2010). To determine RBFOX2-binding sites on transcripts mis-spliced in diabetic mouse hearts, human hg19 RBFOX2 CLIP data (Yeo et al., 2009) were converted to the mm9 mouse genome coordinates using liftOver (Hinrichs et al., 2006). AS events, which displayed an absolute delta Psi > = 0.1 were used for this analysis. The number of events with at least one CLIP peak at a Bayes factor (BF) cutoff of 1 was set as "significant" and BF < 1 was set as "not significant." For RBFOX2-binding cluster analysis, AS events that did not change significantly between all individual comparisons among six samples but exhibited similar expression levels in diabetic hearts were used as controls. Statistical analysis of AS events that were differentially included or excluded in diabetes was determined by calculating a hypergeometric p value of the enrichment of significant AS events, which contained an RBFOX2 CLIP peak in the region of interest, versus the control AS events with RBFOX2 CLIP peaks (Dale et al., 2011; Perez and Granger, 2007; Quinlan and Hall, 2010). Genes with RBFOX2-binding sites were categorized based on their biological or molecular function using the DAVID server (version 6.7) with the whole genome as a background control.

qRT-PCR and Statistical Analysis

qRT-PCR was performed to detect inclusion/exclusion of gene-specific alternative exons and relative mRNA levels. Details are included in the Supplemental Experimental Procedures. Student's t test was used to determine statistical significance between two groups and one-way ANOVA for comparisons of more than two groups with Bonferroni correction using Prism software.

FLAG Immunoprecipitation/Western Blot Analysis

For IP assays, a FLAG IP kit (Sigma FLAGIPT1-1KT) was used to pull down FLAG-tagged WT, DN, or RNA-binding-deficient mutant RBFOX2 expressed in COS M6 or H9c2 cells per the manufacturer's protocol. Precipitated proteins were analyzed on 4%–15% gradient SDS-PAGE gels followed by WB analysis using an anti-FLAG antibody (Ab) conjugated to horseradish peroxidase (HRP) (Sigma A8595), anti-GFP Ab conjugated to HRP (Santa Cruz Biotechnology sc9996), or anti-U1C Ab (Bethyl Laboratories A303-947A).

WB analyses were performed as previously described (Verma et al., 2013). Details are included in the Supplemental Experimental Procedures.

Plasmid Generation

A human RBFOX2 mutant deficient in RNA-binding ($RBFOX2^{RRM}$) was generated by mutating two phenylalanine (F153 and F155) residues necessary for RNA-binding in the RRM into aspartate residues (Auweter et al., 2006; Mayeda et al., 1994; Sun et al., 2012).

ACCESSION NUMBERS

The accession number for the data reported in this paper is GEO: GSE80664.

SUPPLEMENTAL INFORMATION

Supplemental Information includes Supplemental Experimental Procedures and four figures and can be found with this article online at http://dx.doi.org/10.1016/j.celrep.2016.05.002.

AUTHOR CONTRIBUTIONS

C.A.N., S.K.V., V.D., I.J.A., M.J.L., and E.A.J. conducted the experiments; C.A.N. and M.N.K.-M. designed the experiments and wrote the paper. RBFOX2-binding site data analysis was performed by O.B.B. and G.W.Y., calcium data were analyzed by Q.W. and X.H.T.W., chronic chagasic mice were generated and provided by N.J.G., and hypertensive and obese mice were generated and provided by T.I. and A.R.B.

ACKNOWLEDGMENTS

We thank Hong Sun, Yareli Perez, and Rosario Espejo for technical support; Dr. David Konkel for editing the manuscript; Dr. Douglas Black for providing the WT and DN RBFOX2 plasmid DNA constructs; and Dr. Corey Reynolds for his help in quantification of echocardiography data. This work was supported, in part, by a March of Dimes Starter Basil O'Connor Starter Scholar Award (5FY12-21), an American Heart Association Grant (15GRNT22830010), an UTMB Institute for Human Infections and Immunity Mini Center Pilot Award, UTMB pilot grant, and startup funds to M.N.K.-M. This work was supported, in part, by a grant from the NIH/National Institute of Allergy and Infectious Diseases (2RO1AI05478-08) and UTMB Institute for Human Infections and Immunity Mini Center Pilot Award to N.J.G., NIH (UL1TR000071 UTMB CTSA and NIEHS P30 ES006676) grants to A.R.B., a NIH/National Heart, Blood and Lung Institute grant to I.J.A. (5R25HL09636305), and NIH grants (HG0046590 and NS075449) to G.W.Y. G.W.Y. is an Alfred P. Sloan Research Fellow. O.B.B. is a National Defense Science and Engineering Graduate Fellow and NumFOCUS John Hunter Technical Fellow. T.I. was supported by a Ruth L. Kirschstein National Research Service Award from the National Heart Lung Blood Institute (F30HL128036). X.H.T.W. was supported by NIH grants R01-HL089598, R01-HL091947, R01-HL117641, and R41-HL129570 and American Heart Association grant 13EIA14560061.

Received: August 21, 2015
Revised: January 25, 2016
Accepted: April 27, 2016
Published: May 26, 2016

REFERENCES

Aneja, A., Tang, W.H., Bansilal, S., Garcia, M.J., and Farkouh, M.E. (2008). Diabetic cardiomyopathy: insights into pathogenesis, diagnostic challenges, and therapeutic options. Am. J. Med. *121*, 748–757.

Arrington, C.B., Dowse, B.R., Bleyl, S.B., and Bowles, N.E. (2012). Non-synonymous variants in pre-B cell leukemia homeobox (PBX) genes are associated with congenital heart defects. Eur. J. Med. Genet. *55*, 235–237.

Asghar, O., Al-Sunni, A., Khavandi, K., Khavandi, A., Withers, S., Greenstein, A., Heagerty, A.M., and Malik, R.A. (2009). Diabetic cardiomyopathy. Clin. Sci. *116*, 741–760.

Auweter, S.D., Fasan, R., Reymond, L., Underwood, J.G., Black, D.L., Pitsch, S., and Allain, F.H. (2006). Molecular basis of RNA recognition by the human alternative splicing factor Fox-1. EMBO J. *25*, 163–173.

Baraniak, A.P., Chen, J.R., and Garcia-Blanco, M.A. (2006). Fox-2 mediates epithelial cell-specific fibroblast growth factor receptor 2 exon choice. Mol. Cell. Biol. *26*, 1209–1222.

Blackwell, E., Zhang, X., and Ceman, S. (2010). Arginines of the RGG box regulate FMRP association with polyribosomes and mRNA. Hum. Mol. Genet. *19*, 1314–1323.

Boudina, S., and Abel, E.D. (2010). Diabetic cardiomyopathy, causes and effects. Rev. Endocr. Metab. Disord. *11*, 31–39.

Connelly, K.A., Kelly, D.J., Zhang, Y., Prior, D.L., Advani, A., Cox, A.J., Thai, K., Krum, H., and Gilbert, R.E. (2009). Inhibition of protein kinase C-beta by ruboxistaurin preserves cardiac function and reduces extracellular matrix production in diabetic cardiomyopathy. Circ Heart Fail *2*, 129–137.

Dale, R.K., Pedersen, B.S., and Quinlan, A.R. (2011). Pybedtools: a flexible Python library for manipulating genomic datasets and annotations. Bioinformatics *27*, 3423–3424.

Damianov, A., and Black, D.L. (2010). Autoregulation of Fox protein expression to produce dominant negative splicing factors. RNA *16*, 405–416.

Ferrannini, E., and Cushman, W.C. (2012). Diabetes and hypertension: the bad companions. Lancet *380*, 601–610.

Gehman, L.T., Meera, P., Stoilov, P., Shiue, L., O'Brien, J.E., Meisler, M.H., Ares, M., Jr., Otis, T.S., and Black, D.L. (2012). The splicing regulator Rbfox2 is required for both cerebellar development and mature motor function. Genes Dev. *26*, 445–460.

Geraldes, P., and King, G.L. (2010). Activation of protein kinase C isoforms and its impact on diabetic complications. Circ. Res. *106*, 1319–1331.

Gupta, S., Smith, C., Auclair, S., Delgadillo, Ade.J., and Garg, N.J. (2015). Therapeutic efficacy of a subunit vaccine in controlling chronic trypanosoma cruzi infection and Chagas disease is enhanced by glutathione peroxidase over-expression. PLoS ONE *10*, e0130562.

Harcourt, B.E., Penfold, S.A., and Forbes, J.M. (2013). Coming full circle in diabetes mellitus: from complications to initiation. Nat. Rev. Endocrinol. *9*, 113–123.

Hinrichs, A.S., Karolchik, D., Baertsch, R., Barber, G.P., Bejerano, G., Clawson, H., Diekhans, M., Furey, T.S., Harte, R.A., Hsu, F., et al. (2006). The UCSC Genome Browser Database: update 2006. Nucleic Acids Res. *34*, D590–D598.

Huang, S.C., Ou, A.C., Park, J., Yu, F., Yu, B., Lee, A., Yang, G., Zhou, A., and Benz, E.J., Jr. (2012). RBFOX2 promotes protein 4.1R exon 16 selection via U1 snRNP recruitment. Mol. Cell. Biol. *32*, 513–526.

Inoguchi, T., Battan, R., Handler, E., Sportsman, J.R., Heath, W., and King, G.L. (1992). Preferential elevation of protein kinase C isoform beta II and diacylglycerol levels in the aorta and heart of diabetic rats: differential reversibility to glycemic control by islet cell transplantation. Proc. Natl. Acad. Sci. USA *89*, 11059–11063.

Jangi, M., Boutz, P.L., Paul, P., and Sharp, P.A. (2014). Rbfox2 controls autoregulation in RNA-binding protein networks. Genes Dev. *28*, 637–651.

Katz, Y., Wang, E.T., Airoldi, E.M., and Burge, C.B. (2010). Analysis and design of RNA sequencing experiments for identifying isoform regulation. Nat. Methods *7*, 1009–1015.

Kirkpatrick, L.L., McIlwain, K.A., and Nelson, D.L. (1999). Alternative splicing in the murine and human FXR1 genes. Genomics *59*, 193–202.

Liu, Q., Chen, X., Macdonnell, S.M., Kranias, E.G., Lorenz, J.N., Leitges, M., Houser, S.R., and Molkentin, J.D. (2009). Protein kinase Calpha, but not PKCbeta or PKCgamma, regulates contractility and heart failure susceptibility: implications for ruboxistaurin as a novel therapeutic approach. Circ. Res. *105*, 194–200.

Liu, Y., Lei, S., Gao, X., Mao, X., Wang, T., Wong, G.T., Vanhoutte, P.M., Irwin, M.G., and Xia, Z. (2012). PKCβ inhibition with ruboxistaurin reduces oxidative stress and attenuates left ventricular hypertrophy and dysfunction in rats with streptozotocin-induced diabetes. Clin. Sci. *122*, 161–173.

Lorenzo, O., Urbé, S., and Clague, M.J. (2006). Systematic analysis of myotubularins: heteromeric interactions, subcellular localisation and endosome related functions. J. Cell Sci. *119*, 2953–2959.

Lovci, M.T., Ghanem, D., Marr, H., Arnold, J., Gee, S., Parra, M., Liang, T.Y., Stark, T.J., Gehman, L.T., Hoon, S., et al. (2013). Rbfox proteins regulate

Please cite this article in press as: Nutter et al., Dysregulation of RBFOX2 Is an Early Event in Cardiac Pathogenesis of Diabetes, Cell Reports (2016), http://dx.doi.org/10.1016/j.celrep.2016.05.002

alternative mRNA splicing through evolutionarily conserved RNA bridges. Nat. Struct. Mol. Biol. *20*, 1434–1442.

Mayeda, A., Munroe, S.H., Cáceres, J.F., and Krainer, A.R. (1994). Function of conserved domains of hnRNP A1 and other hnRNP A/B proteins. EMBO J. *13*, 5483–5495.

Mientjes, E.J., Willemsen, R., Kirkpatrick, L.L., Nieuwenhuizen, I.M., Hoogeveen-Westerveld, M., Verweij, M., Reis, S., Bardoni, B., Hoogeveen, A.T., Oostra, B.A., and Nelson, D.L. (2004). Fxr1 knockout mice show a striated muscle phenotype: implications for Fxr1p function in vivo. Hum. Mol. Genet. *13*, 1291–1302.

Monica, K., Galili, N., Nourse, J., Saltman, D., and Cleary, M.L. (1991). PBX2 and PBX3, new homeobox genes with extensive homology to the human proto-oncogene PBX1. Mol. Cell. Biol. *11*, 6149–6157.

Mora, S., and Pessin, J.E. (2000). The MEF2A isoform is required for striated muscle-specific expression of the insulin-responsive GLUT4 glucose transporter. J. Biol. Chem. *275*, 16323–16328.

Nakahata, S., and Kawamoto, S. (2005). Tissue-dependent isoforms of mammalian Fox-1 homologs are associated with tissue-specific splicing activities. Nucleic Acids Res. *33*, 2078–2089.

Naya, F.J., Black, B.L., Wu, H., Bassel-Duby, R., Richardson, J.A., Hill, J.A., and Olson, E.N. (2002). Mitochondrial deficiency and cardiac sudden death in mice lacking the MEF2A transcription factor. Nat. Med. *8*, 1303–1309.

Perez, F., and Granger, B.E. (2007). IPython: a system for interactive scientific computing. Comput. Sci. Eng. *9*, 21–29.

Quinlan, A.R., and Hall, I.M. (2010). BEDTools: a flexible suite of utilities for comparing genomic features. Bioinformatics *26*, 841–842.

Stankunas, K., Shang, C., Twu, K.Y., Kao, S.C., Jenkins, N.A., Copeland, N.G., Sanyal, M., Selleri, L., Cleary, M.L., and Chang, C.P. (2008). Pbx/Meis deficiencies demonstrate multigenetic origins of congenital heart disease. Circ. Res. *103*, 702–709.

Sun, S., Zhang, Z., Fregoso, O., and Krainer, A.R. (2012). Mechanisms of activation and repression by the alternative splicing factors RBFOX1/2. RNA *18*, 274–283.

Taguchi-Atarashi, N., Hamasaki, M., Matsunaga, K., Omori, H., Ktistakis, N.T., Yoshimori, T., and Noda, T. (2010). Modulation of local PtdIns3P levels by the PI phosphatase MTMR3 regulates constitutive autophagy. Traffic *11*, 468–478.

Tieu, B.C., Lee, C., Sun, H., Lejeune, W., Recinos, A., 3rd, Ju, X., Spratt, H., Guo, D.C., Milewicz, D., Tilton, R.G., and Brasier, A.R. (2009). An adventitial IL-6/MCP1 amplification loop accelerates macrophage-mediated vascular inflammation leading to aortic dissection in mice. J. Clin. Invest. *119*, 3637–3651.

Trachanas, K., Sideris, S., Aggeli, C., Poulidakis, E., Gatzoulis, K., Tousoulis, D., and Kallikazaros, I. (2014). Diabetic cardiomyopathy: from pathophysiology to treatment. Hellenic J. Cardiol. *55*, 411–421.

Venables, J.P., Brosseau, J.P., Gadea, G., Klinck, R., Prinos, P., Beaulieu, J.F., Lapointe, E., Durand, M., Thibault, P., Tremblay, K., et al. (2013a). RBFOX2 is an important regulator of mesenchymal tissue-specific splicing in both normal and cancer tissues. Mol. Cell. Biol. *33*, 396–405.

Venables, J.P., Lapasset, L., Gadea, G., Fort, P., Klinck, R., Irimia, M., Vignal, E., Thibault, P., Prinos, P., Chabot, B., et al. (2013b). MBNL1 and RBFOX2 cooperate to establish a splicing programme involved in pluripotent stem cell differentiation. Nat. Commun. *4*, 2480.

Verma, S.K., Deshmukh, V., Liu, P., Nutter, C.A., Espejo, R., Hung, M.L., Wang, G.S., Yeo, G.W., and Kuyumcu-Martinez, M.N. (2013). Reactivation of fetal splicing programs in diabetic hearts is mediated by protein kinase C signaling. J. Biol. Chem. *288*, 35372–35386.

Wang, L., Fan, C., Topol, S.E., Topol, E.J., and Wang, Q. (2003). Mutation of MEF2A in an inherited disorder with features of coronary artery disease. Science *302*, 1578–1581.

Wei, C., Qiu, J., Zhou, Y., Xue, Y., Hu, J., Ouyang, K., Banerjee, I., Zhang, C., Chen, B., Li, H., et al. (2015). Repression of the central splicing regulator RBFox2 is functionally linked to pressure overload-induced heart failure. Cell Rep. *10*, 1521–1533.

Weng, L., Kavaslar, N., Ustaszewska, A., Doelle, H., Schackwitz, W., Hébert, S., Cohen, J.C., McPherson, R., and Pennacchio, L.A. (2005). Lack of MEF2A mutations in coronary artery disease. J. Clin. Invest. *115*, 1016–1020.

Whitman, S.A., Cover, C., Yu, L., Nelson, D.L., Zarnescu, D.C., and Gregorio, C.C. (2011). Desmoplakin and talin2 are novel mRNA targets of fragile X-related protein-1 in cardiac muscle. Circ. Res. *109*, 262–271.

Yeo, G.W., Coufal, N.G., Liang, T.Y., Peng, G.E., Fu, X.D., and Gage, F.H. (2009). An RNA code for the FOX2 splicing regulator revealed by mapping RNA-protein interactions in stem cells. Nat. Struct. Mol. Biol. *16*, 130–137.

Zhu, B., Ramachandran, B., and Gulick, T. (2005). Alternative pre-mRNA splicing governs expression of a conserved acidic transactivation domain in myocyte enhancer factor 2 factors of striated muscle and brain. J. Biol. Chem. *280*, 28749–28760.